

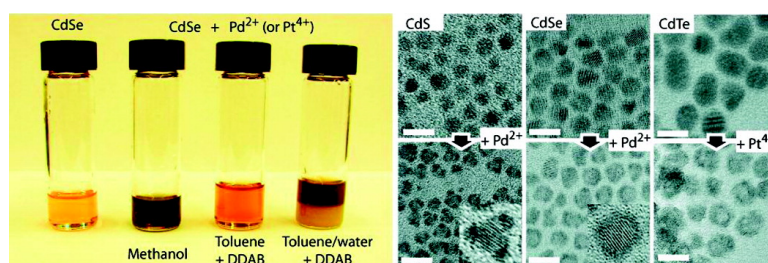
Article

Effects of Ion Solvation and Volume Change of Reaction on the Equilibrium and Morphology in Cation-Exchange Reaction of Nanocrystals

Stacey E. Wark, Chih-Hao Hsia, and Dong Hee Son

J. Am. Chem. Soc., **2008**, 130 (29), 9550-9555 • DOI: 10.1021/ja802187c • Publication Date (Web): 28 June 2008

Downloaded from <http://pubs.acs.org> on February 8, 2009



More About This Article

Additional resources and features associated with this article are available within the HTML version:

- Supporting Information
- Access to high resolution figures
- Links to articles and content related to this article
- Copyright permission to reproduce figures and/or text from this article

[View the Full Text HTML](#)

Effects of Ion Solvation and Volume Change of Reaction on the Equilibrium and Morphology in Cation-Exchange Reaction of Nanocrystals

Stacey E. Wark, Chih-Hao Hsia, and Dong Hee Son*

Department of Chemistry, Texas A&M University, College Station, Texas 77842

Received March 24, 2008; E-mail: dhson@mail.chem.tamu.edu

Abstract: The effects of cation solvation and the volume change (ΔV) of reaction on the equilibrium and the morphology change in the cation-exchange reactions of metal chalcogenide nanocrystals, $\text{CdE} \rightarrow \text{M}_x\text{E}_y$ ($\text{E} = \text{S}, \text{Se}, \text{Te}$; $\text{M} = \text{Pd}, \text{Pt}$), were investigated. Since the solvation of cations is an important controllable factor determining the free energy of the reaction, the effect of varying cation solvation conditions on the equilibrium of the reaction was examined. A two-phase solvent environment, where the cations involved in the exchange reaction were preferentially solvated in different phases by using selective cation complexing molecules, was particularly efficient in increasing the thermodynamic driving force. The effect of ΔV of reaction on the morphology of the product nanocrystals was also investigated. Depending on the stress developed in the lattice during the reaction, product nanocrystals underwent varying degrees of morphological changes such as void formation and fragmentation in addition to the preservation of the original morphology of the reactant nanocrystals. The knowledge of the effect of ion solvation and ΔV of reaction on the equilibrium and product morphology provides a new strategy and useful guides to the application of cation-exchange reactions for the synthesis of a broader range of inorganic nanocrystals.

1. Introduction

Chemical modification of nanocrystalline solids via diffusion or exchange of atoms has recently been demonstrated to be a simple and versatile way to create a variety of inorganic nanostructures.^{1–7} Cation-exchange reaction in ionic nanocrystals, in particular, has been shown to be very useful for transforming ionic nanocrystals into other ionic nanocrystals, hetero-interfaced and periodic superlattice nanostructures.^{1,4,8} For instance, complete transformation of CdSe into Ag₂Se nanocrystals was achieved in less than a second simply by mixing a CdSe nanocrystal solution with a silver salt solution at room temperature.⁹ The reaction could also be made completely reversible to recover CdSe from Ag₂Se through the law of mass action. Such fast kinetics and reversibility of the reaction are considered to be mainly due to the lower activation barrier for the diffusion of atoms in nanocrystalline solids compared to the bulk phase.

In principle, the high efficiency of the cation-exchange reaction in nanocrystals can be extended more broadly to exchange reactions with other cations or possibly even anions, which provides new or complementary synthetic routes to a variety of nanocrystals.^{10–13} Ultimately, the efficiency of the cation-exchange reaction as a synthetic method will depend on the thermodynamic driving force and the activation barrier. In order to utilize the cation-exchange reaction as a versatile synthetic method of nanocrystals, it will be important to understand and perhaps control the factors affecting the kinetics and thermodynamics of the reaction other than temperature and concentration. Since the net reaction involves the exchange of two cations, solvation of cations is an important factor determining the thermodynamics of the reaction. Cation solvation can be controlled to a certain extent by varying the solvent environment, which will influence the overall thermodynamics of the reaction. In the simplest case, one could vary the solvation condition by changing the polarity of the solvent. Consideration of the factors affecting the activation barrier is a bit more complicated. The activation barrier for the diffusion and exchange of the cations will depend on many factors, such as the structure of the anion sublattice, the ionicity of the cation–anion interaction, and the structural difference between the reactant and product phases. Among these factors, the

- (1) Son, D. H.; Hughes, S. M.; Yin, Y.; Alivisatos, A. P. *Science* **2004**, *306*, 1009–1012.
- (2) Mokari, T.; Aharoni, A.; Popov, I.; Banin, U. *Angew. Chem., Int. Ed.* **2006**, *45*, 8001–8005.
- (3) Yin, Y.; Rioux, R. M.; Erdonmez, C. K.; Hughes, S.; Somorjai, G. A.; Alivisatos, A. P. *Science* **2004**, *304*, 711–714.
- (4) Camargo, P. H. C.; Lee, Y. H.; Jeong, U.; Zou, Z.; Xia, Y. *Langmuir* **2007**, *23*, 2985–2992.
- (5) Jeong, U.; Kim, J.-U.; Xia, Y.; Li, Z.-Y. *Nano Lett.* **2005**, *5*, 937–942.
- (6) Dloczik, L.; Koenenkamp, R. *Nano Lett.* **2003**, *3*, 651–653.
- (7) Schaak, R. E.; Sra, A. K.; Leonard, B. M.; Cable, R. E.; Bauer, J. C.; Han, Y.-F.; Means, J.; Teizer, W.; Vasquez, Y.; Funck, E. S. *J. Am. Chem. Soc.* **2005**, *127*, 3506–3515.
- (8) Robinson, R. D.; Sadtler, B.; Demchenko, D. O.; Erdonmez, C. K.; Wang, L.-W.; Alivisatos, A. P. *Science* **2007**, *317*, 355–358.
- (9) Chan, E. M.; Marcus, M. A.; Fakra, S.; ElNaggar, M.; Mathies, R. A.; Alivisatos, A. P. *J. Phys. Chem. A* **2007**, *111*, 12210–12215.

- (10) Koktysh, D. S.; McBride, J. R.; Dixit, S. K.; Feldman, L. C.; Rosenthal, S. J. *Nanotechnology* **2007**, *18*, 495607/495601–495607/495604.
- (11) Malik, M. A.; O'Brien, P.; Revaprasadu, N. *J. Mater. Chem.* **2002**, *12*, 92–97.
- (12) Yang, Z.; Smetana, A. B.; Sorensen, C. M.; Klabunde, K. J. *Inorg. Chem.* **2007**, *46*, 2427–2431.
- (13) Jiang, X. C.; Mayers, B.; Wang, Y. L.; Cattle, B.; Xia, Y. N. *Chem. Phys. Lett.* **2004**, *385*, 472–476.

structural difference between the reactant and product phases is the most easily quantifiable factor and bears additional importance concerning the morphology change of the nanocrystals after the reaction. Morphology change of the nanocrystals, especially when the reaction accompanies a large change in the volume or lattice parameters, can be an important issue when the initial reactant nanocrystals are used as the structural template.^{1,6,14}

In this work, we investigated the effect of solvent environment and volume change of the reaction on the equilibrium and efficiency of the cation-exchange reaction and the morphology change in the product nanocrystals. The studied cation-exchange reactions are $\text{CdE} \rightarrow \text{M}_x\text{E}_y$, ($\text{E} = \text{S}, \text{Se}, \text{Te}$; $\text{M} = \text{Pd}, \text{Pt}$), occurring under ambient conditions. The fractional volume change ($\Delta V/V$) of reaction ranges from -0.25 to -0.46 , based on bulk lattice parameters.^{15–19} For all the reactions studied, the equilibrium of the reaction was strongly dependent on the variation of the solvent environment, which modified the thermodynamics of the reaction by changing the cation solvation condition. In particular, a two-phase solvent environment, where the two cations involved in the exchange reaction were separated in different phases, strongly favored the forward reaction. This clearly indicates the importance of the cation solvation by solvent medium in determining the thermodynamic driving force and therefore the efficiency of the reaction. While all the reactions studied were slower than the reaction $\text{CdSe} \rightarrow \text{Ag}_2\text{Se}$, the activation barrier was still sufficiently low for the reaction to occur even at ambient temperature. These results suggest the possibility of applying various selective cation complexing reagents, more commonly used in organic reactions (e.g., crown ether), to enhance the efficiency of the ion-exchange reactions of nanocrystals. Relatively large $\Delta V/V$ of the reaction had varying degrees of effects on the morphology of the product nanocrystals. Void formation and fragmentation as well as the preservation of the original morphology were observed, depending on the degree of lattice stress developed in the product nanocrystals during the reaction.

2. Experimental Section

Triethylphosphine oxide-passivated, spherical nanocrystals of CdS, CdSe, and CdTe were synthesized following the well-established solvothermal methods using CdO and elemental S, Se, and Te dissolved in coordinating solvents as precursors.^{20,21} CdSe rods were synthesized following the procedure developed by Peng et al.²² All the nanocrystals used in the cation-exchange reactions were dispersed in toluene.

For the cation-exchange reaction, PdCl_2 and PtCl_4 were used as the source of cations. Three different reaction conditions that provided different cation solvation environments were used as described in Table 1. The reactions occurred in a single-phase solvent environment under conditions A and B, and in a two-phase solvent environment under condition C. Didodecyldimethylammo-

Table 1. Reaction Conditions and Solvent Environments for Cation-Exchange Reaction between Cd Chalcogenide Nanocrystals (CdE) and Metal Chloride (MCl_n)

	conditions		
	A	B	C
CdE	toluene, 2.5 mL	toluene, 0.10 mL	toluene, DDAB, 2 mL
MCl_n	methanol, 0.5 mL	toluene, DDAB, 1.9 mL	water, 1 mL

nium bromide (DDAB) used in conditions B and C provided the metal salts solubility in toluene, probably by forming a DDA–metal halide complex.²³ In a simple extraction experiment, approximately 1 equiv of DDAB was needed to extract 1 equiv of metal ion from aqueous phase to organic phase. Typical concentrations of the nanocrystals (CdE formula unit base) and metal salts (MCl_n) in the final reaction mixture were approximately 0.1 and 5 mM, respectively.

All the reactions were performed by mixing the nanocrystal solution with the metal salt solution under ambient conditions. The reaction time was varied from a few minutes to several hours, depending on the specific reaction conditions. After the reaction, the product nanocrystals were precipitated by adding methanol and centrifuging the reaction mixture. The recovered nanocrystals were rinsed with methanol for further characterization of their structure and composition. The lattice structures of the reactant and product nanocrystals were examined by taking powder X-ray diffraction (XRD) patterns of the dried samples on a Bruker-AXS GADDS diffractometer. Transmission electron micrographs (TEM) of the nanocrystals were acquired using a JEOL 2010 transmission electron microscope. For in situ study of the structure of the thermally annealed nanocrystals, TEM and electron diffraction patterns of the nanocrystal samples on Si_3N_4 substrate were recorded before and after heating. The elemental composition of the nanocrystals was obtained from energy dispersive X-ray (EDX) analysis employing an Oxford Instruments INCA EDX system. The oxidation state of Pd and Pt cations in the product phase was determined from X-ray photoelectron spectroscopy (XPS, Kratos Axis Ultra).

3. Results and Discussion

3.1. Effect of Solvent on the Equilibrium. To investigate the effect of cation solvation conditions on the equilibrium of the cation-exchange reaction, three different reaction conditions were used, as described in Table 1. Under condition A, metal cations were solvated by a small amount of methanol homogeneously mixed with toluene. The same condition was used for the reaction $\text{CdSe} \rightarrow \text{Ag}_2\text{Se}$ in earlier studies.^{1,8} Under condition B, both metal cations and reactant nanocrystals were in the toluene phase. Under condition C, Pd and Pt cations were initially in the aqueous phase. During the reaction, DDAB transported Pd and Pt cations into the toluene phase, while the exchanged Cd cations were solvated in the aqueous phase.

When comparable total concentrations of the reactants were used, cation exchange was the most efficient under condition C, followed by conditions A and B, for all the reactions investigated in this study. Figure 1 shows photographs of the reaction mixtures (CdSe nanocrystal and Pd salt solution) taken several minutes after the reactants were mixed under conditions A–C. The difference in the extent of reaction can be seen from the colors of the reaction mixtures, since the initial color of CdSe nanocrystal turns dark brown as the reaction proceeds.

(14) Henkes, A. E.; Schaak, R. E. *Chem. Mater.* **2007**, *19*, 4234–4242.

(15) Weinstein, M.; Wolff, G. A.; Das, B. N. *Appl. Phys. Lett.* **1965**, *6*, 73–75.

(16) Traill, R. J.; Boyle, R. W. *Am. Mineral.* **1955**, *40*, 555–559.

(17) Groenvold, F.; Haraldsen, H.; Kjekshus, A. *Acta Chem. Scand.* **1960**, *14*, 1879–1893.

(18) Geller, S. *Acta Crystallogr.* **1962**, *15*, 713–721.

(19) Villars, P., Ed. *ASM Alloy Phase Diagrams Center*; ASM International: Materials Park, OH, 2007; <http://www.asminternational.org/AsmEnterprise/APD>.

(20) Peng, Z. A.; Peng, X. *J. Am. Chem. Soc.* **2001**, *123*, 183–184.

(21) Reiss, P.; Bleuse, J.; Pron, A. *Nano Lett.* **2002**, *2*, 781–784.

(22) Peng, X.; Manna, U.; Yang, W.; Wickham, J.; Scher, E.; Kadavanich, A.; Allvisatos, A. P. *Nature* **2000**, *404*, 59–61.

(23) Elliot, D. J.; Furlong, D. N.; Gengenbach, T. R.; Grieser, F.; Urquhart, R. S.; Hoffman, C. L.; Rabolt, J. F. *Colloids Surf., A* **1995**, *103*, 207–219.

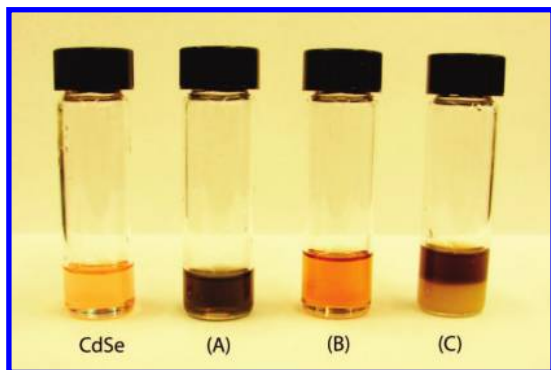


Figure 1. Photographs of the reaction mixtures under the conditions A–C described in Table 1.

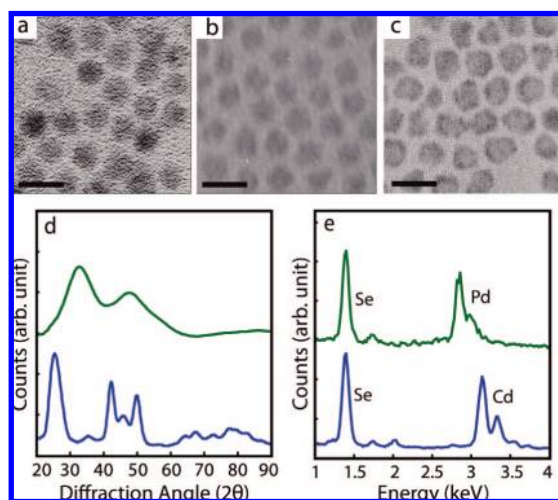


Figure 2. TEM images of (a) reactant CdSe nanocrystals, (b) fully cation-exchanged product PdSe, and (c) partially cation-exchanged PdSe nanocrystals from the reaction $\text{CdSe} \rightarrow \text{PdSe}$. Scale bars are 10 nm. (d) XRD patterns and (e) EDX spectra of CdSe (blue) and PdSe (green) nanocrystals.

For the reaction $\text{CdSe} \rightarrow \text{PdSe}$ with 5 nm CdSe nanocrystals, the reaction completed on the order of 10 min under condition C. Under condition A, the product often precipitated with only partial cation exchange during the same reaction time. Condition B resulted in the lowest extent of reaction among the three reaction conditions.

Figure 2a–c compares the TEM images of the reactant and product nanocrystals for the reaction $\text{CdSe} \rightarrow \text{PdSe}$ under conditions A and C, where the partially and fully cation-exchanged nanocrystals were formed, respectively. Completion of the cation exchange was confirmed by XRD and EDX analysis (Figure 2d,e). In the case of full cation-exchange reaction, the exchange ratio between Cd and Pd cations was approximately 1:1, based on the EDX measurement. For partially exchanged nanocrystals (Figure 2c), only the outer surface of the nanocrystal was exchanged, while maintaining the 1:1 exchange ratio of the cations.

It is relatively easy to understand the differences in the efficiency of the cation-exchange reaction under different solvent medium conditions. Under condition C, DDAB acts as the phase-transfer catalyst selectively for Pd cations, bringing the CdSe nanocrystal and Pd cation into the same phase. Pd and Pt cations are known to form a DDA–metal halide complex via quaternary nitrogen, which gives solubility in nonpolar solvents.²³ Transfer of Pd and Pt cations from the aqueous to the

organic phase occurred within seconds after shaking the reaction mixture, which was easily seen from the disappearance of the color of metal ions in the aqueous phase. On the other hand, the exchanged Cd cations were solvated preferentially in the aqueous phase, separate from the product nanocrystals in the organic phase, since DDAB does not complex with Cd cations efficiently.²⁴ Such a condition should provide a strong thermodynamic driving force for the forward reaction, consistent with the most effective reaction observed under condition C.

Under condition A, the advantage of isolating Cd cations from the product nanocrystals and Pd or Pt cations via selective solvation does not exist. Methanol provides a favorable condition for solvating all ionic species present in the reaction mixture. The equilibrium of the reaction will depend on the relative stability of cations solvated by the same medium in addition to the relative thermodynamic stability of the reactant and product nanocrystals. Under condition B, nonpolar solvent medium disfavors the solvation of Cd cations, while Pd and Pt cations can exist stably in nonpolar solvent with the help of DDAB. Inefficient reaction under condition B is probably due to the unfavorable conditions for solvation of Cd cations. However, adding a few drops of methanol or water into the reaction mixture of condition B immediately shifted the equilibrium to the forward direction by creating a reaction condition similar to C. These observations clearly demonstrate the importance of cation solvation conditions in determining the thermodynamic driving force and efficiency of the reaction. Considering that typical solvation energy of divalent cations in aqueous medium is about -400 kcal/mol,²⁵ the strong dependence of the equilibrium on cation solvation conditions is not unexpected.

The immediate shift of the equilibrium upon a small change in the solvent environment discussed above also confirms a relatively low activation barrier of the cation-exchange reaction in nanocrystals. However, the reaction $\text{CdSe} \rightarrow \text{PdSe}$ exhibited much slower kinetics compared to $\text{CdSe} \rightarrow \text{Ag}_2\text{Se}$ studied earlier, suggesting a higher activation barrier.⁹ To further examine the reversibility of the reaction, an attempt was made to induce the reverse reaction $\text{PdSe} \rightarrow \text{CdSe}$. In the case of Ag_2Se , the reverse reaction was completed within a minute when an excess of Cd cations was added to the solution of Ag_2Se nanocrystals under ambient conditions. When PdSe nanocrystals were put under the same reaction conditions, the reverse reaction was not observed, even after several hours of reaction time, confirming the higher activation barrier than in the case of Ag_2Se . Cation-exchange reactions of CdS and CdTe with Pd and Pt cations exhibited the same trend of solvent-dependent equilibrium as observed in the reaction $\text{CdSe} \rightarrow \text{PdSe}$. However, the reactions were generally faster in the order of telluride to sulfide. Completion of the reaction $\text{CdTe} \rightarrow \text{PdTe}$ occurred in several minutes, while $\text{CdS} \rightarrow \text{PdS}$ required ~ 1 h of reaction time under condition C.

3.2. Morphology of the Partially Cation-Exchanged Nanocrystals. In previous cation-exchange reactions of the nanocrystals, the anisotropic morphology of the nanocrystals was often preserved after the reaction.^{1,6,14} This indicates that the frame of the anion sublattice was maintained with only minor adjustments of the anion positions, while cations were completely exchanged. In this case, the reaction can be viewed as the diffusion of cations through the anion sublattice that has a

(24) In a separate measurement, the partition ratio of Cd^{2+} ions in toluene and water (1:1 volume ratio) was 1:6 in the presence of DDAB, as determined from ICP-MS.

(25) Marcus, Y. *J. Chem. Soc., Faraday Trans.* **1991**, *87*, 2995–2999.

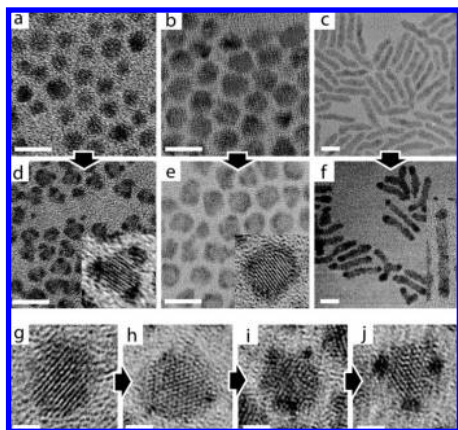


Figure 3. TEM images of (a–c) reactant and (d–f) partially cation-exchanged product nanocrystals from the reactions $\text{CdE} \rightarrow \text{PdE}$ ($\text{E} = \text{S}$ or Se). (a–c) Images of CdS sphere, CdSe sphere, and CdSe rod, respectively. (d–f) Images of the products from (a–c), respectively. Insets in (d–f) are high-resolution images of the product nanocrystals in each panel. Scale bars in (a–f) are 10 nm. (g–j) High-resolution TEM images showing the progression of the cation exchange on zinc blende CdS nanocrystals with Pt cations. Scale bars in (g–j) are 2 nm.

limited flexibility. Two interesting questions arise: Where on the nanocrystal does the exchange of cations initiate, and how does the reaction propagate? To address this question, intermediate structures with partial cation exchange were investigated. Partially cation-exchanged products were obtained by precipitating and washing the product nanocrystals before the completion of the reaction.

Figure 3a–f compares TEM images of the partially Pd-exchanged nanocrystals produced from CdS and CdSe spheres and CdSe rods. In the case of zinc blende CdS nanocrystals (Figure 3a,d), the regions of the reaction on the nanocrystals coincide with the apexes of the tetragonal pyramid. Exchange with Pt cations also resulted in the partially Pt-exchanged nanocrystals of the same morphology. Figure 3g–j shows the progression of the exchange reaction in zinc blende CdS nanocrystals by Pt cations. XRD patterns of partially exchanged nanocrystals show only the peaks originating from the unexchanged part of the nanocrystals (see Supporting Information). Interestingly, the shape of the nanocrystals becomes more faceted as the reaction continues. On the other hand, partial cation exchange occurred homogeneously on the outer surface of the sphere in the case of wurtzite CdSe nanocrystals (Figure 3b,e), in contrast to CdS nanocrystals. In wurtzite CdSe nanorods (Figure 3c,f), the reaction occurred preferentially at both ends of the rod under condition A, while the preference was weakened under condition C. These observations clearly demonstrate that the initiation and progress of the cation-exchange reaction depends on the lattice structure and morphology of the reactant nanocrystals.

Preferential reaction at the tip of the CdSe nanorods is reminiscent of the formation of the semiconductor nanorods by solvothermal methods or reduction of gold at the tip of the semiconductor nanorods.^{22,26} The anisotropic reaction to form nanorods has been explained in terms of different accessibility of reactant monomer to the different regions of the nanocrystals due to the selective passivation of particular faces of the lattice by the surfactant molecules.²² The difference in polarity in the

nanocrystal facets has also been discussed as a factor inducing selective deposition of metal in the case of cubic PbS nanocrystals.²⁷ An analogous argument may be made to explain the preferential exchange reaction at a particular region of the nanocrystals observed in this study. In combination with the steric factor described above, generally higher reactivity at the regions with higher surface curvature and lower coordination number may also have played a role in determining the preferred site for the initiation of the reaction.²⁸ Formation of the partially Pd- and Pt-exchanged zinc blende CdS nanocrystals, where the reaction occurred at the four apexes of the tetragon, may be explained in this way.

3.3. Structure and Morphology of the Fully Cation-Exchanged Nanocrystals. Figure 4 compares the morphologies of the initial reactant and fully cation-exchanged product nanocrystals from the reactions $\text{CdE} \rightarrow \text{M}_x\text{E}_y$ ($\text{E} = \text{S}$, Se , Te ; $\text{M} = \text{Pd}$, Pt). The reactions are categorized into three groups according to the nature of the morphology change, as will be discussed in detail below.

To characterize the lattice structure of the fully cation-exchanged nanocrystals, XRD patterns of the reaction products were obtained. Figure 5 compares the XRD patterns of the reactant (blue) and product (green) phases. However, the identification of the lattice structures of the product phase from the XRD patterns alone was not straightforward due to the very broad diffraction peaks and the existence of multiple phases of Pd and Pt chalcogenides.

For Pd-exchanged nanocrystals, the exchange ratio between Pd and Cd cations obtained from EDX measurements was approximately 1:1, indicating the average oxidation state of 2+ for Pd. Based on this result, the expected phases of the product nanocrystals are PdS, PdSe, and PdTe, which adopt tetragonal, tetragonal, and hexagonal structure, respectively, in the bulk phase. Considering the very broad diffraction peaks, it is likely that the product is in a disordered state of the corresponding bulk phase. The similarity of the experimental XRD patterns of PdS and PdSe nanocrystals to the theoretical XRD patterns, calculated using their bulk lattice parameters with the extra peak broadening introduced (Figure 6), further supports the above conclusion. For the simulation of the XRD patterns, PowderCell (Windows version 2.4) was used with Gaussian broadening function to best-fit the experimental peak widths.²⁹ In the case of Pt-exchanged nanocrystals, the cation-exchange ratio and the oxidation state of Pt cations in the product phase measured from XPS were more complex (see Supporting Information). For sulfide, the oxidation state of Pt cations was 2+, consistent with the observed Pt:S ratio of 1:1 in the product nanocrystals. In telluride, Pt cations exhibited mixed oxidation states of 2+ and 4+, indicating a more heterogeneous nature of the composition and structure.

If all the cation-exchange reactions considered here produce stoichiometric products with bulk equilibrium structures, $\Delta V/V$ of the reaction should range from -0.25 to -0.46 , as shown in Table 2. In comparison, $\Delta V/V$ for $\text{CdSe} \rightarrow \text{Ag}_2\text{Se}$ studied earlier is only 0.06, with very little ($<1\%$) change in the lattice parameters.^{1,8} In principle, a decrease in volume and/or a change in the shape of the product nanocrystals should be seen, based on the theoretical values of $\Delta V/V$. However, the TEM images

(26) Mokari, T.; Rothenberg, E.; Popov, I.; Costi, R.; Banin, U. *Science* **2004**, *304*, 1787–1790.

(27) Yang, J.; Elim, H. I.; Zhang, Q.; Lee, J. Y.; Ji, W. *J. Am. Chem. Soc.* **2006**, *128*, 11921–11926.

(28) Kudera, S.; Carbone, L.; Casula, M. F.; Cingolani, R.; Falqui, A.; Snoeck, E.; Parak, W. J.; Manna, L. *Nano Lett.* **2005**, *5*, 445–449.

(29) Kraus, W.; Nolze, G. *J. Appl. Crystallogr.* **1996**, *29*, 301–302.

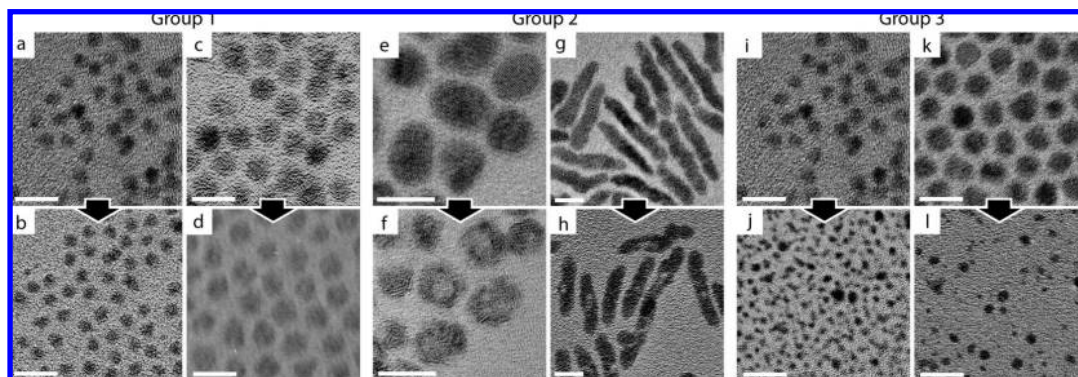


Figure 4. TEM images of the reactant CdE (E = S, Se, Te) and fully exchanged product nanocrystals. Reactant–product pair is indicated by an arrow connecting the two panels: (a→b) CdS→PdS, (c→d) CdSe→PdSe, (e→f) CdTe→PtTe, (g→h) CdSe→PdSe, (i→j) CdS→PtS, and (k→l) CdSe→PtSe. Scale bars are 10 nm.

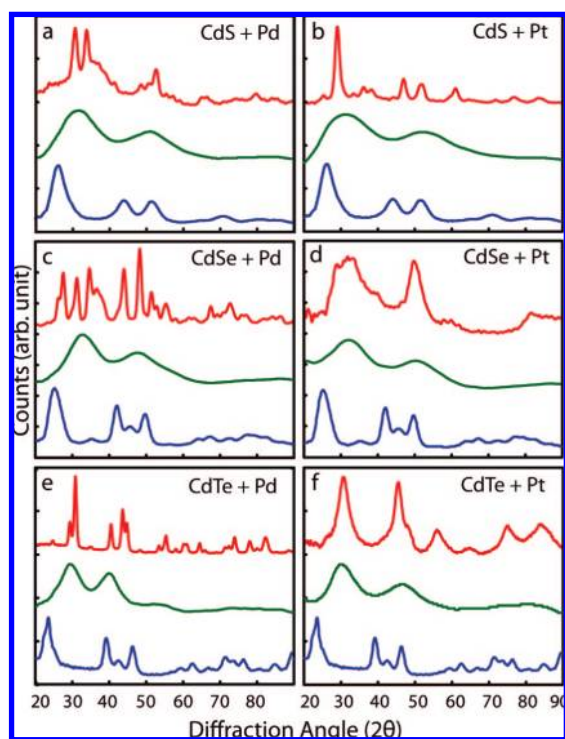


Figure 5. XRD patterns of reactant (blue), product (green), and thermally annealed product (red) nanocrystals from the cation-exchange reaction $\text{CdE} \rightarrow \text{M}_x\text{E}_y$ (E = S, Se, Te; M = Pd, Pt). Reactant nanocrystals and exchanging metal ions are indicated in each panel.

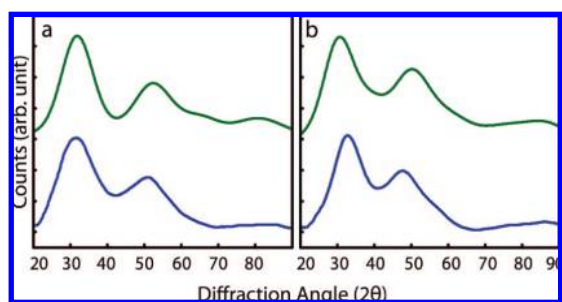


Figure 6. Experimental (blue) and simulated (green) XRD patterns of the fully cation-exchanged (a) PdS and (b) PdSe nanocrystals.

in Figure 4 show varying degrees of morphology changes, depending on the reaction and the size of the nanocrystals.

Table 2. Structure, Lattice Parameter, and Fractional Volume Change of Reaction ($\Delta V/V$) for the Reactant and Possible Product Phases

material	structure	lattice parameters	$\Delta V/V$
CdS	zinc blende	$a = 5.82$	reactant
PdS	tetragonal	$a = 6.43, c = 6.61$	-0.30
PtS	tetragonal	$a = 3.47, c = 6.10$	-0.25
PtS ₂	rhombohedral	$a = 3.54, c = 5.04$	-0.44
CdSe	wurtzite	$a = 4.30, c = 7.01$	reactant
PdSe	tetragonal	$a = 6.73, c = 6.91$	-0.30
Pd ₁₇ Se ₁₅	cubic	$a = 10.61$	-0.29
PtSe ₂	rhombohedral	$a = 3.73, c = 5.08$	-0.45
Pt ₅ Se ₄	monoclinic	$a = 6.58, b = 4.61, c = 11.12$	-0.27
CdTe	wurtzite	$a = 4.57, c = 7.44$	reactant
PdTe	hexagonal	$a = 4.13, c = 5.66$	-0.38
PtTe	monoclinic	$a = 6.87, b = 3.96, c = 7.04$	-0.33
Pt ₂ Te ₃	monoclinic	$a = 6.93, b = 4.00, c = 17.12$	-0.42
PtTe ₂	hexagonal	$a = 4.03, c = 5.22$	-0.46

In group 1, the product phase retains the original morphology. This is observed in the reaction of small CdS and CdSe nanocrystals with Pd ions. $\Delta V/V$ for these reactions is approximately -0.3 . In the case of the reaction $\text{CdSe} \rightarrow \text{PdSe}$ (Figure 4c→d), contraction of the plane perpendicular to the c -axis by about 30% is the major change of the structure.¹⁹ However, contraction of the volume corresponding to such a structural change is not apparent in the TEM images. It is possible that the product phase is kinetically frozen in a disordered and metastable state, where the lattice stress is sustained without conforming to the equilibrium lattice structure.

In group 2, a void is formed inside the nanocrystals. This is observed in PdSe (Figure 4g→h) and PtTe (Figure 4e→f), especially for larger nanocrystals. The void formation may be explained in terms of the release of the stress in the lattice accumulated in the product phase during the reaction.³⁰ The stress that was sustainable during the early phase of the reaction may have reached a critical point, which triggered the formation of the void from the interior, releasing the stress in the lattice. Although the formation of the void is seemingly analogous to the Kirkendall effect observed in earlier studies of Co_xS_y nanocrystals,³ the origin of the void formation is different. In the case of the Kirkendall effect, void formation is driven by the disparity of the diffusion coefficients of the two chemical

(30) Suh, Y. S.; Park, D. G.; Jang, S. A. *Thin Solid Films* **2004**, *450*, 341–345.

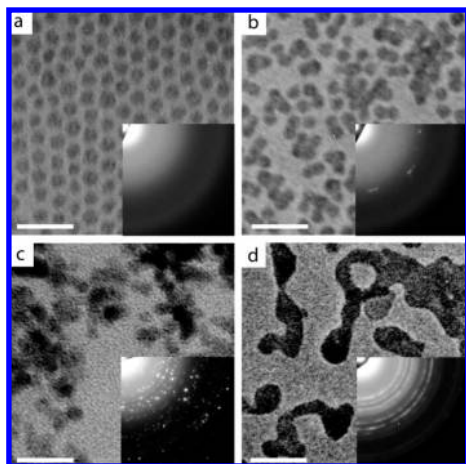


Figure 7. TEM images of in situ PdSe nanocrystals under different in situ heating conditions: (a) unheated, (b) 150 °C for 20 min, (c) 200 °C for 20 min, and (d) 600 °C for 10 min. Insets are the electron diffraction patterns for each sample. Scale bars are 20 nm.

species propagating in the opposite direction. However, in the case of the cation-exchange reaction, it is the static anion sublattice that determines the morphology of the nanocrystals after the reaction.

In group 3, fragmentation of the nanocrystals to smaller pieces occurred. This was observed in the reactions of CdS and CdSe nanocrystals with Pt cations (Figure 4 i→j and k→l). Fragmentation may have resulted from continuous break-off of the ion-exchanged parts from the main body of the reacting nanocrystal due to the excessive lattice mismatch at the hetero-interface.

3.4. Structure of the Thermally Annealed Product Nanocrystals. As discussed above, the product nanocrystals from cation-exchange reaction may have a significant lattice stress and disorder, especially when the product nanocrystals did not conform to the expected change of volume. In that case, the product nanocrystals may transform to the thermodynamically more stable and ordered phase via thermal annealing of the lattice. To see if the metastable and disordered structure of the reaction product can relax to a more equilibrated structure, an in situ TEM measurement of the thermally annealed product nanocrystals was made. Thermal annealing was done by heating the nanocrystal sample deposited on thin Si₃N₄ substrate in situ on the temperature-controlled sample holder of the TEM. The sample was heated at several different temperatures. The TEM images and electron diffraction patterns of the thermally annealed sample were taken after the sample stage cooled to ambient temperature. Figure 7 shows the TEM images and electron diffraction patterns of PdSe nanocrystals before and after thermal annealing. After heating at 150 °C for 20 min (Figure 7b), the nanocrystals exhibit a noticeable reduction in size compared to the unannealed PdSe nanocrystals (Figure 7a). This is consistent with our assumption that thermal annealing will lead to a more equilibrated structure of the product phase with $\Delta V/V = -0.3$. However, the structure of the lattice still seems disordered, based on the lack of well-defined diffraction patterns.

After further heating at 200 °C for 20 min, the nanocrystals began to form a crystalline phase with increasing extent of

agglomeration (Figure 7c). The electron diffraction pattern in Figure 7c corresponds to Pd₁₇Se₁₅. With continued heating at a higher temperature, the nanocrystals melted completely. The diffraction pattern obtained after cooling to ambient temperature clearly shows the diffraction rings corresponding to Pd₁₇Se₁₅ (Figure 7d). However, it is not entirely clear if the transformation to Pd₁₇Se₁₅ is purely structural annealing or chemical disproportionation. In the bulk phase, PdSe can disproportionate into Pd₁₇Se₁₅ and PdSe₂ above ~600 °C.³¹ What is observed in Figure 7c,d may be the combined result of structural annealing and disproportionation. Ex situ thermal annealing of PdSe nanocrystals in octadecene at 200 °C for 30 min also yielded Pd₁₇Se₁₅ nanocrystals. However, the annealed nanocrystals were much larger than the original PdSe nanocrystals due to the agglomeration. Other reaction products also exhibited agglomeration and crystallization to more equilibrated structure upon ex situ heating. XRD patterns of the ex situ heated samples are shown in Figure 5 (red curve in each panel). Crystalline tetragonal PdS and PtS were formed upon thermal annealing of the disordered product nanocrystals. Heating of PdSe resulted in Pd₁₇Se₁₅, as described above. Thermal annealing of the disordered PdTe resulted in mixed phases of PdTe and PdTe₂.

4. Conclusion

We have shown that the equilibrium of the cation-exchange reaction in nanocrystals can be significantly changed by modifying the cation solvation conditions of the solvent medium. In particular, the equilibrium of the cation-exchange reaction could be shifted toward the formation of the product via selective solvation of cations in a particular solvent phase. The effect of a large volume change of reaction on the morphology of the product phase has also been studied. This is a particularly important issue when the reactant nanocrystal acts as a morphological template. Depending on the stress developed in the lattice during the reaction due to the difference in the lattice structure between the reactant and the product, the product nanocrystals underwent varying degrees of morphological changes, such as void formation and fragmentation. The knowledge of the effects of ion solvation and ΔV of reaction on the equilibrium and product morphology obtained from this study provides a new strategy and useful guides to the application of cation-exchange reactions for the synthesis of a broader range of inorganic nanocrystals.

Acknowledgment. This work was supported by Texas A&M University (TAMU). We thank the Microscopy and Imaging Center of TAMU and Dr. Zhiping Luo for assistance in obtaining in situ temperature-controlled TEM. We would also like to thank the Materials Characterization Facility and Elemental Analysis Laboratory of TAMU for XPS and ICP-MS measurements.

Supporting Information Available: XPS data of Pd and Pt chalcogenide nanocrystals obtained from cation-exchange reaction and XRD of partially exchanged PdSe. This material is available free of charge via the Internet at <http://pubs.acs.org>.

JA802187C

(31) Okamoto, H. *J. Phase Equilib. Diffus.* **1992**, *13*, 69–72.